

Effect of end plates on lateral torsional buckling loads of steel beams in ambient and fire conditions

Marco Santarelli, Markku Heinisuo, and Ari Aalto

Summary. The effect of three dimensional behaviors of the structural steel joints on the behaviors of the steel members is rather open question in the literature. In this paper the effects of the end plates on the lateral torsional buckling loads of steel beams both in the ambient and in the fire conditions are considered. Two simple problems are solved to enable the estimations of the joint stiffness to the buckling loads in more complicated problems. The solutions for the one span beams with double symmetric I-shaped cross-sections can be used in many practical cases as references. The solutions are derived using commercial finite element method programs and the comparisons are done with the analytical solutions when available in the literature. The material models in the fire are those appearing in the most novel European standards for steel structures. The results show the increase of 5-20 % in the buckling loads using typical (10-20 mm) end plates. The buckling loads can be 1.4-1.7 times larger if the end plates are very thick, or generally the joint stiffness in warping is large, compared to the case without end plates. The situation is the same both in ambient and fire situations. The parameter kL was found to be the proper measure when considering different buckling modes. In the cases considered the lateral torsional buckling mode was critical if $kL > 2$. If this parameter is very large, then the role of warping is decreasing, as is known generally. The considerable increases in the resistance times can be got using the thermal analysis instead of the analysis where the steel temperatures are supposed to be the same in all points of the cross-section. The criteria to stop the calculations in the thermal analysis are still open.

Key words: steel beams, joint stiffness, lateral torsional buckling, fire

Introduction

The effect of three dimensional behaviors of the structural steel joints on the behaviors of the steel members is rather open question for many cases in the literature. Some considerations especially for welded joints can be found.

The theory for the elastic lateral torsional buckling theory can be considered as well-known referring to three pioneer works [1], [2] and [3]. The behavior of steel joints in three dimensions has been considered by studying how the actions are transferred from the steel member to another in [4], [5] and [6]. The effect of warping joint stiffness on the stability problems has been considered in [7]. The reference [8] includes an excellent summary and the state of the art dealing with the behavior of the structural steel joints in three dimensions up today, but warping and bimoments are not considered in that reference.

It is clear, that to study the effects of the behavior of the joints on the behavior of the entire frame system, then the entire joint layout should be known, as is the case in Refs. [4]-[8]. However, they must use new joints, which have not been used before, in almost

every practical project. So the designers need some information how the joints may affect to the behavior of distinct parts of the frame. In the German standards for steel structures [9], [10] are given factors to consider the effects of warping and “weak” direction rotational stiffness on the lateral torsional buckling loads of beams.

In the present paper one simple case is presented to demonstrate the effects of the warping constraints on the lateral buckling load of a beam. The idea is to show, what mean physically the warping constraints in one case, and how much they have effect on the buckling load. It is hoped, that the results of this study can be used by the designers to estimate the effects of more complicated joints on the lateral torsional buckling loads of beams. This is important in practical cases, because typically the design programs do not include the finite elements including warping degree of freedoms, although these have been known from 1970’s. So they cannot solve eigenvalue problems including lateral torsional problems in practice.

In a recent paper [11] is shown how the joint stiffness can be taken into account when considering the flexural buckling of the column in two directions. In the present paper will be studied the effect of the end plates welded on both flanges and on web of a double symmetric I-profile at both ends of the beam. The effects of the end plates on the elastic lateral torsional buckling loads of simply supported beams are considered. Two loading cases are studied: the point load in the middle point of the beam and the uniform load acting at the centroid of the cross-section along the entire length of the beam. The component method application as in [11] will be studied in the further studies.

The calculations in the present paper are done both in ambient and in fire conditions. In fire, both the simplified conservative analysis where the steel temperatures are the same at every points of the cross-section, and the thermal analysis, will be considered. The material models in the fire are those appearing in the most novel European standards for steel structures [12]. In fire the standard ISO fire is considered.

The calculations are done applying commercial finite element method programs. Most of the calculations are done using COMSOL program [13] and some check calculations are done using ABAQUS program [14]. The results are compared to the analytical results when available in the literature. Linear buckling loads and geometrical non-linear cases are considered. Thermal analysis in fire included large displacements in the model.

The solutions of these simplified cases may be used as references for the members with more complicated joint configurations, such as bolted beam to column joints with extended end plates and similar cases.

Analytic solutions without end plates in ambient and fire conditions

Consider the simply supported one span beam with span length L . The coordinate system is shown in Fig. 1. The x -axis is in the axial direction, y -axis bending means the bending around the “strong” axis and z -axis bending means the bending around the “weak” axis of the I-beam. The web is in the vertical position, in z -direction. The loads are acting in z -direction, see Fig. 1.

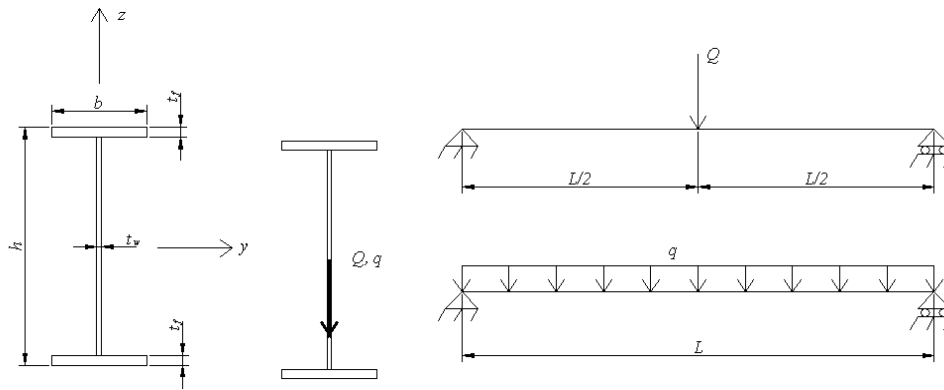


Figure 1. Coordinate system and notations for the cross-section dimensions.

The simple supports mean typical fork supports at the both ends of the beam. At the supports the displacements in y and z directions are prevented. The rotation around the x -axis is prevented (torsional support). The rotations around y - and z -axis as well the warping are free to happen at supports.

The profile of the beam is a double symmetric and in this case the dimensions of IPE profiles without rounded corners are used to represent welded profiles with the same dimensions. The concentrated load Q is acting at the mid point of the beam, meaning in the centroid of the cross-section and at the mid-span of the beam. The uniform load q is also acting in the centroid of the cross-section and it is acting along the entire length of the beam.

The material properties of steel are used following [15] and [16]. This means elastic modulus $E = 210000$ MPa and Poisson's ratio $\nu = 0.3$. The elastic modulus is decreasing at elevated temperatures as given in [16]. It is supposed, that the Poisson's ratio for steel is constant at elevated temperatures.

The bending moments at the mid sections of the beams are for the concentrated load and for the uniform load:

$$M_Q = \frac{1}{4}QL \Rightarrow Q = 4\frac{M}{L} \quad (1)$$

$$M_q = \frac{1}{8}qL^2 \Rightarrow q = 8\frac{M}{L^2} \quad (2)$$

The critical bending moments for the lateral torsional buckling for both cases can be calculated approximatively for many kinds of boundary conditions and for many loadings with different moment diagrams. In this paper the method appearing in the US codes [17] derived originally by Kirby and Nethercot [18] is used to calculate the analytical results.

The lateral torsional buckling moments can be presented as follows for the simply supported beam with the double symmetric cross-section [17]:

$$M_{cr,Q,q} = C_{b,Q,q} \frac{\pi}{L} \sqrt{EI_z GI_t \left(1 + \frac{EI_\omega}{GI_t} \left(\frac{\pi}{L} \right)^2 \right)} \quad (3)$$

$$C_{b,Q} = 1.316 \quad (4a)$$

$$C_{b,q} = 1.136 \quad (4b)$$

where I_z is the second moment of area about z-axis, I_ω is the warping constant, I_t is the St. Venant's torsional constant, G is the shear modulus,

$$G = \frac{E}{2(1+\nu)} \quad (5)$$

The factor C_b in Eqs. (3)-(4) is named in [17]: lateral torsional buckling modification factor for non-uniform moment diagrams when both ends of the unsupported segment are braced. If this factor is 1.0 then the result is the exact for the uniform moment along the beam.

The cross-sectional quantities needed to calculate the critical moments from Eqs. (3) and (4) and further critical loads from Eqs. (1) and (2) are for double symmetrical I-cross-section and using the notations of Figure 1:

$$I_z = \frac{1}{6} t_f b^3 + \frac{1}{12} (h - 2t_f) t_w^3 \quad (6)$$

$$I_\omega = \frac{1}{4} I_z (h - t_f)^2 \quad (7)$$

$$I_t = \frac{1}{3} [2bt_f^3 + (h - t_f) t_w^3] \quad (8)$$

Using the notation for the torsional parameter:

$$k = \sqrt{\frac{GI_t}{EI_\omega}} \quad (9)$$

then the critical moments (3) and (4) can be presented as

$$M_{cr,Q} = 1.316 \frac{\pi}{L} \sqrt{EI_z GI_t \left(1 + \left(\frac{\pi}{kL} \right)^2 \right)} \quad (10)$$

$$M_{cr,q} = 1.136 \frac{\pi}{L} \sqrt{EI_z GI_t \left(1 + \left(\frac{\pi}{kL} \right)^2 \right)} \quad (11)$$

The following limit values can be obtained

$$\lim_{kL \rightarrow \infty} M_{cr,Q} = 1.316 \frac{\pi}{L} \sqrt{EI_z GI_t} \quad (12)$$

$$\lim_{kL \rightarrow \infty} M_{cr,q} = 1.136 \frac{\pi}{L} \sqrt{EI_z GI_t} \quad (13)$$

These values can be considered as St. Venant critical moments.

In the Table 1 are given the initial data for two cross-sections and corresponding cross-sectional quantities.

Table 1. Initial data for two cross-sections.

	h (mm)	b (mm)	t_f (mm)	t_w (mm)	I_z (mm ⁴)	I_ω (mm ⁶)	I_t (mm ⁴)
“IPE200”	200	100	8.5	5.6	$1.419 \cdot 10^6$	$1.299 \cdot 10^{10}$	$5.215 \cdot 10^4$
“IPE500”	500	200	16	10.2	$2.137 \cdot 10^7$	$1.249 \cdot 10^{12}$	$7.173 \cdot 10^5$

Now the critical loads Q_{cr} and q_{cr} can be calculated, if the span of the beam is given. In the Figures 2-5 are shown the critical loads for two cases, uniform load and concentrated load. There are also given the critical loads corresponding to St. Venant critical moments and the loads corresponding to initial yielding moments if the material strength of the beam is 500 MPa and calculated based on Eqs. (2)- (3) and data of Table 1. For “IPE200” the span where the lateral torsional buckling is more critical compared to the start of the yield is about 2.2-2.4 m. For “IPE500” this span is about 3.8-4.3 m. If the yield strength is smaller, then these limit spans are a little bit longer.

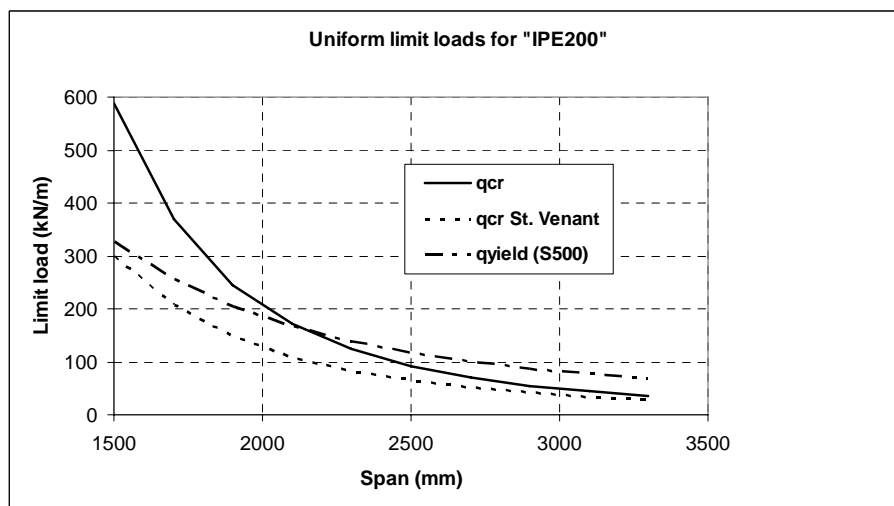


Figure 2. Uniform limit loads for “IPE200”.

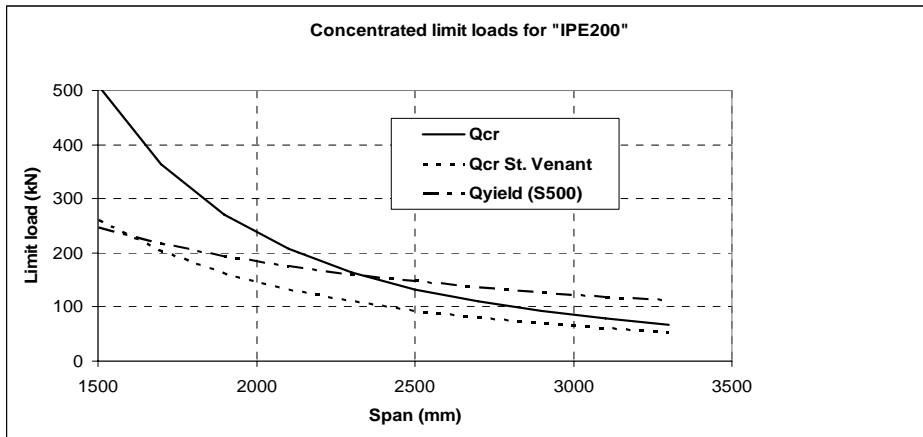


Figure 3. Concentrated limit loads for "IPE200".

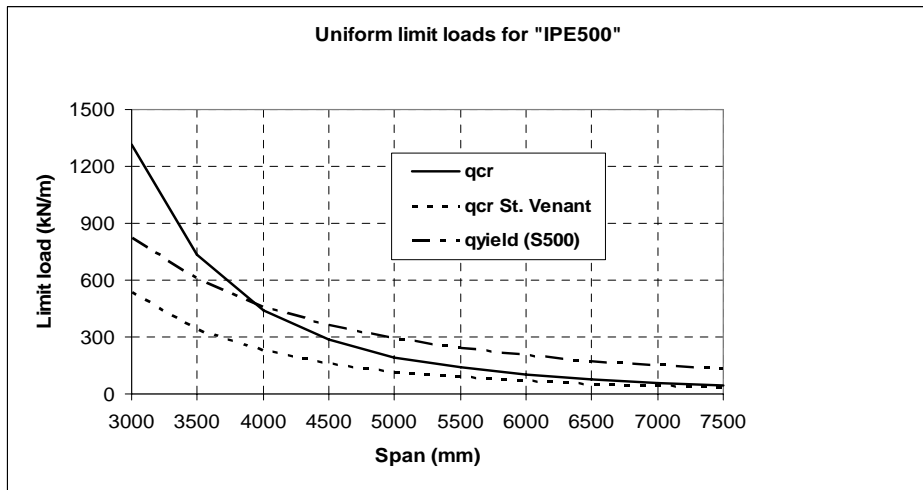


Figure 4. Uniform limit loads for "IPE500".

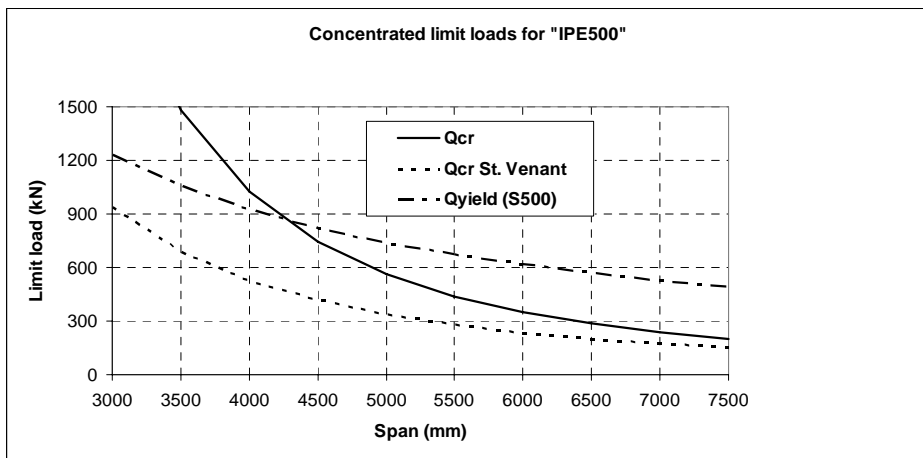


Figure 5. Concentrated limit loads for "IPE500".

Table 2. Spans L and kL values for two cross-sections.

“IPE200”	L (m)	1	2	3	4	5	6	7
	kL	1.24	2.49	3.73	4.97	6.21	7.46	8.70
“IPE500”	L (m)	3	4	5	6	7	8	9
	kL	1.41	1.88	2.35	2.82	3.29	3.76	4.23

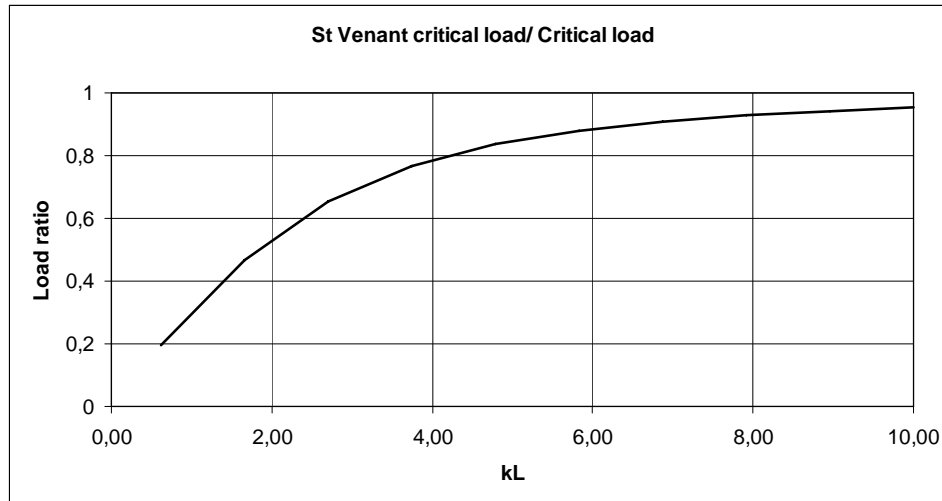


Figure 6. Critical load ratios.

The comparisons for the lateral torsional cases are more convenient to do using a non-dimensional torsional parameter kL , instead of the span L . The relationships are given in Table 2 between the spans and the parameters kL for two cross-sections considered.

In Figure 6 is shown the critical ratios of St. Venant critical loads to the critical lateral torsional loads versus the torsional parameter. The relationships are the same for both cross-sections and for both load cases considered in this paper.

It can be seen, that the values of our interest are in the range of about $kL > 1.8$, “IPE200”: span larger than about 2.8 m and “IPE500”: span larger than about 3.8 m. In this range the St Venant solution give low (conservative) critical loads, so the warping stiffness is essential to take into consideration in this range. It will be shown in the following section, that in the range say $kL < 2$, the critical buckling modes are something else but the lateral torsional modes.

Consider next the same cases in fire. Consider the situation, where the steel temperatures are the same in every point of the cross-section of the beam, which is the conservative assumption for most of the fire cases. This case is named as “uniform temperature profile analysis” in the following. The structural system of the one span simply supported beam does not change in fire. The critical moments are calculated using Eqs. (10) - (11). These are in fire

$$M_{cr,Q,fi} = 1.316 \frac{\pi}{L} E_{fi} \sqrt{\frac{I_z I_t}{2(1+\nu)} \left(1 + \left(\frac{\pi}{kL} \right)^2 \right)} \quad (14)$$

$$M_{cr,q,fi} = 1.136 \frac{\pi}{L} E_{fi} \sqrt{\frac{I_z I_t}{2(1+\nu)} \left(1 + \left(\frac{\pi}{kL} \right)^2 \right)} \quad (15)$$

because only quantity which is changing at elevated temperatures is the elastic modulus of steel. It is supposed, that the Poisson's ratio does not change at elevated temperatures.

This means, that the lateral buckling loads are reduced in fire conditions similarly as the elastic modulus of steel due to elevated temperatures. In this study it is supposed, that the elastic modulus of steel is reduced following the standard EN 1993-1-2 [16]. The reduction of the elastic modulus is given in the reference [16] as follows:

$$E_{fi} = k_{E,\theta} E \quad (16)$$

where $k_{E,\theta}$ is the reduction function (≤ 1) depending on the steel temperature θ .

The lateral buckling loads in fire temperatures can be calculated using the following equations

$$Q_{cr,fi} = k_{E,\theta} Q_{cr} \quad (17)$$

$$q_{cr,fi} = k_{E,\theta} q_{cr} \quad (18)$$

provided that the steel temperature is the same at every cross-section of the beam. It should be noted, too, that the limiting span, when the lateral torsional buckling is the critical collapse mode compared e.g. to the yield, is smaller than in the ambient conditions, because the elastic modulus is reduced more than the yield strength at the elevated temperatures.

The reductions of the elastic modulus and the yield strengths are shown in Figure 7 as a function of the steel temperature based on [16].

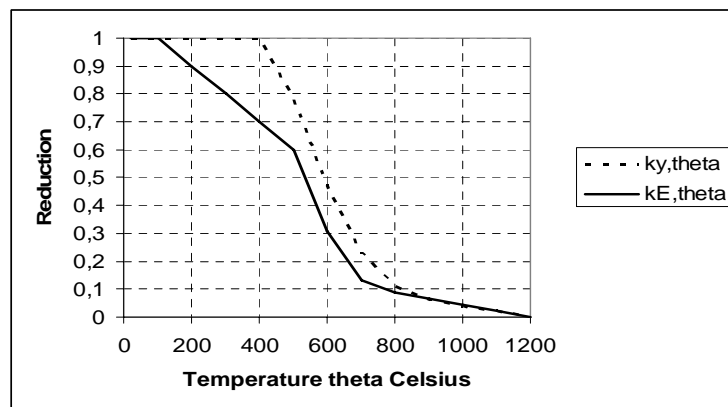


Figure 7. Reduction of elastic modulus and yield strength in fire [16].

Finite element models

In order to estimate the effects of the end plates on the lateral torsional loads given above the finite element models were made for those calculations, because no results were found in the literature dealing with the effects of the end plates on these critical loads. In this study no analytical approach will be proposed for the end plate cases. The finite element models were calibrated against the analytical results given above.

The program used in most of the calculations was COMSOL Multiphysics 3.2 [13]. Some check calculations were done using the program ABAQUS STANDARD 6.9 [14].

The models in COMSOL were made using 3D brick elements. A standard meshes for the orthogonal slices were used. In the longitudinal direction were used different length elements depending on the span of the beam but anyway calculated to produce at least a brick every 200 mm in the x-direction. For “IPE200” beam with the concentrated load and the span 4 m the critical loads changed only about 1 % if the brick element length varied from 200 to 40 mm, so the results calculated using the brick length 200 mm are reliable in this sense. The main meshing scheme for COMSOL is shown in Fig. 8.

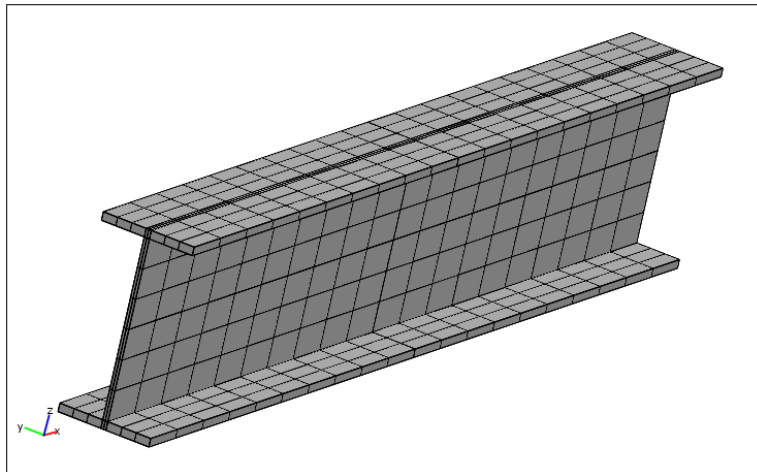


Figure 8. Meshing scheme for COMSOL models.

In the modeling, a particular attention was given to the boundary conditions to simulate a simply supported beam. After various attempts the half of the beam span was modeled. It was found that no anti-symmetric buckling modes with the respect of the mid cross-section of the beam were active in the range of the beams considered.

The following constraints were used:

- Mid cross-section of the beam:
All longitudinal displacements are prevented (Fig. 9 a).
- Fork support:
Bottom horizontal edge, vertical displacements are prevented (Fig. 9 b),
Central vertical edge, horizontal displacements are prevented (Fig. 9 b).

The joint constraints are illustrated in Fig 9.

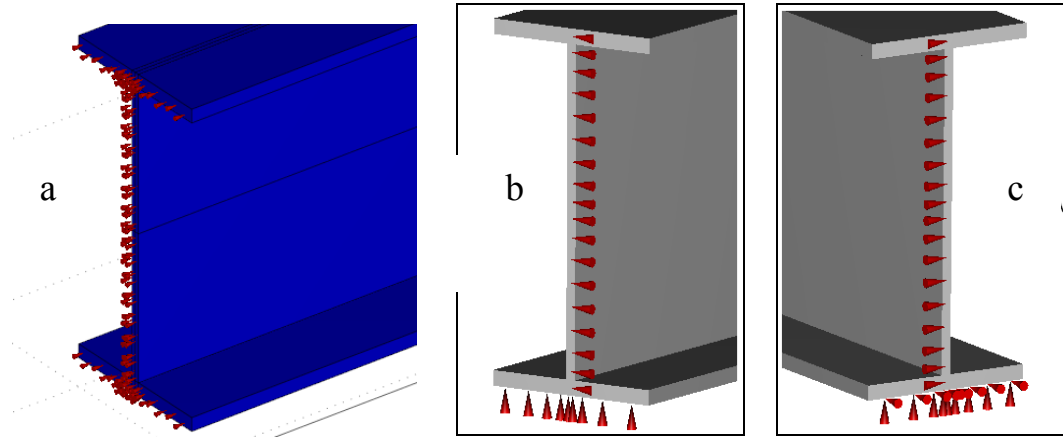


Figure 9. Constraints at supports.

Some comparisons were done by modeling the entire beam and using the fork support at the other beam end as shown in Fig. 9 b. At the other end were extra constraints at the bottom flange for warping and for the rotation around the “weak” axis, as shown in Fig. 9 c. Without end plates the difference between this joint and the fork support may not be large. But if there is the thick end plate at this support, then this joint starts to behave like warping and “weak” axis rotation totally prevented.

The entire beams with the loads are illustrated in Figure 10. Note, that only halves of these beams were modeled in the most of the cases. The entire beams were modeled only in the cases with the constraints as shown in Fig. 9 c at the other end.

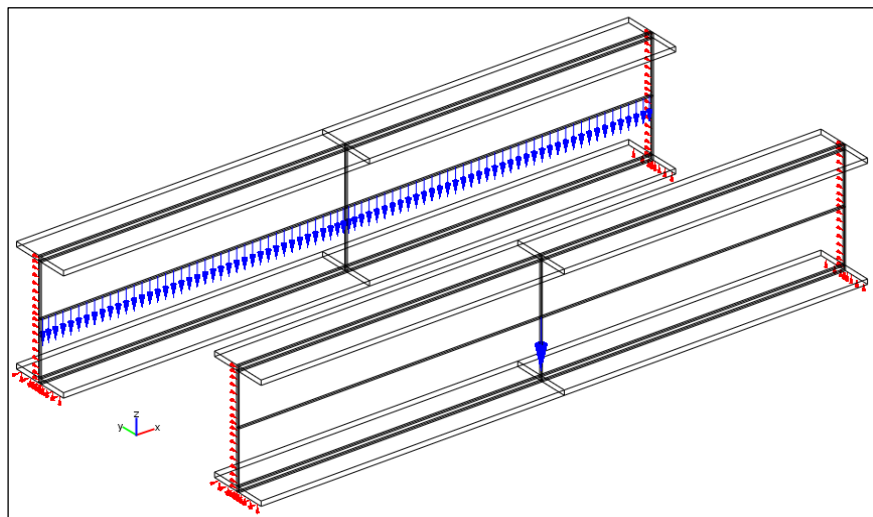


Figure 10. Beam models.

The ABAQUS models were made using the four node shell elements with similar meshing as in COMSOL.

The buckling loads were calculated in the range $kL \approx 1-5$. The buckling loads were calculated using the linear buckling modules of the programs using the linear material model in the ambient conditions. Figure 11 presents the critical uniform loads in the ambient conditions for “IPE200” beam.

It can be seen, that especially in the range $kL > 2$ the COMSOL and ABAQUS results are near each others. Figure 12 presents the results for the same beam with concentrated load at the mid-point.

Figure 13 and 14 illustrate the critical loads calculated by the finite element models and these are compared to the analytical solutions in the ambient conditions.

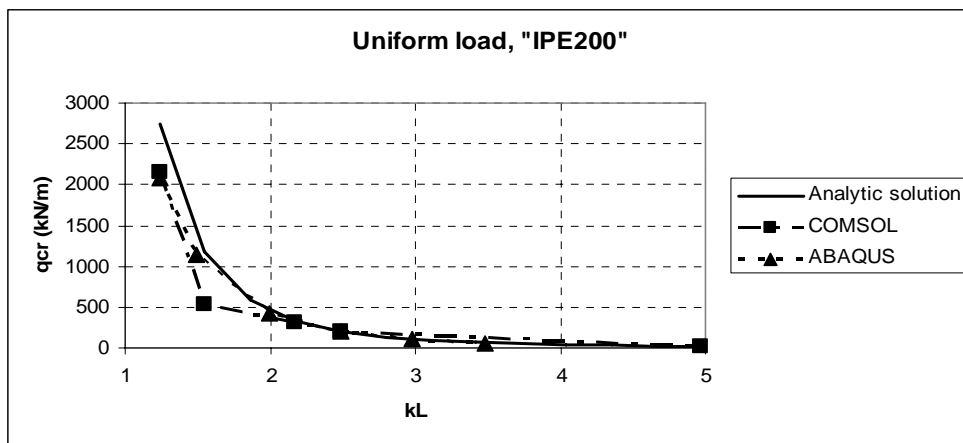


Figure 11. Critical uniform loads in ambient conditions.

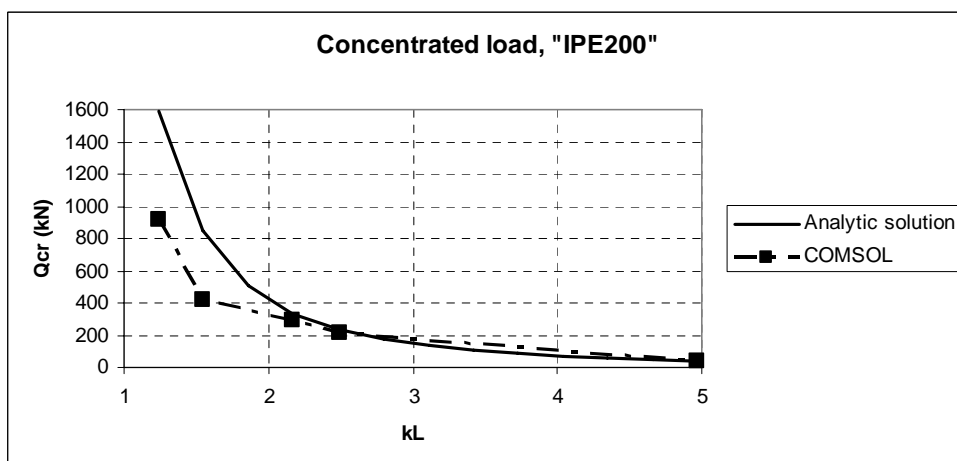


Figure 12. Critical concentrated loads in ambient conditions.

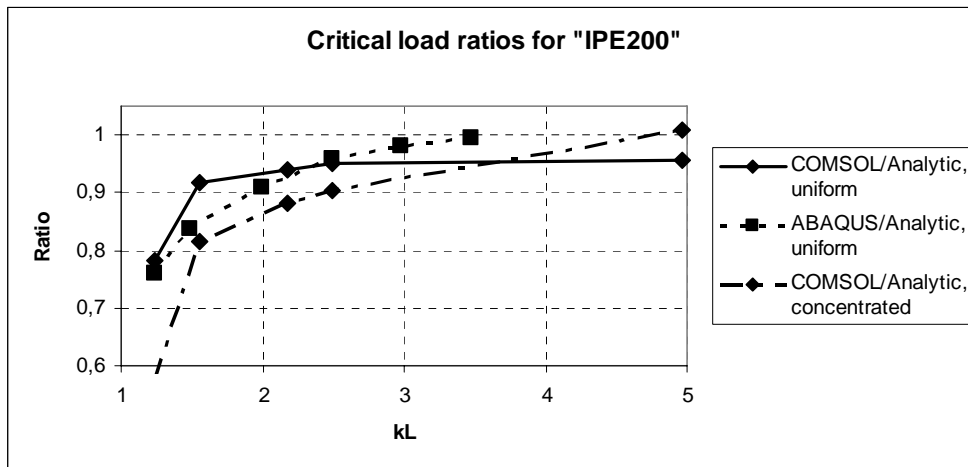


Figure 13. Critical load ratios for “IPE200”.

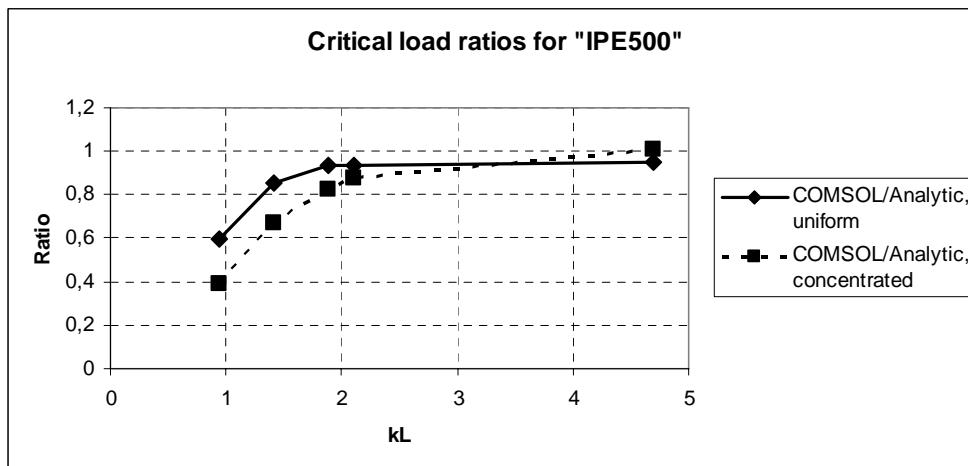


Figure 14. Critical load ratios for “IPE500”.

It can be seen, that the critical loads calculated by the finite element methods are decreasing compared to the analytical solutions when the parameter kL is getting below about 2.0. Figure 15 illustrates the lowest buckling modes in COMSOL analysis for three cases for the half of the beam.

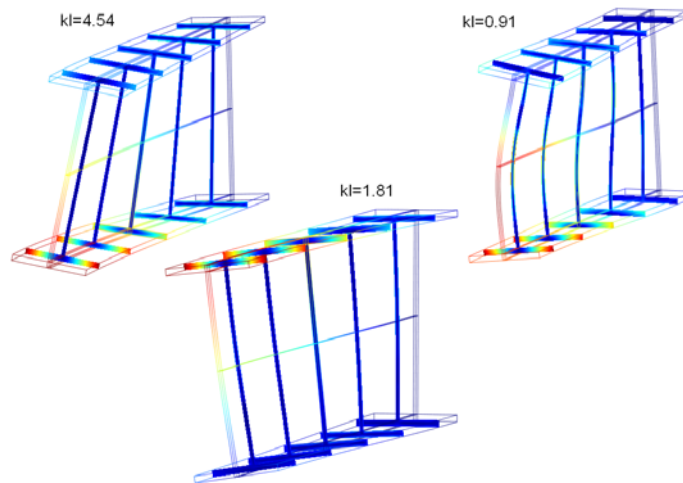


Figure 15. Buckling modes with three different parameters kL for “IPE500”, uniform load.

It can be seen, that:

- With small values ($kL < 1$) local buckling modes near the supports are critical.
- In the range about $kL = 1.0 - 2.0$ distortional buckling modes are critical.
- After that ($kL > 2.0$) the lateral buckling modes without local or distortional buckling modes are critical.

This was observed in all the cases considered. Similar trends were found for two “HEA” typed welded profiles, too (“HEA200”, “HEA500”). The limits for different buckling modes are not strict and some mixing of modes may appear. However, the trends for different buckling modes were as given above.

At elevated temperatures the analytical solutions were calculated using the Eqs. (14) and (15). The COMSOL results were compared to those. In Fig. 16 are compared the ratios of the critical loads at different temperatures. It can be seen, that the ratios follow very exactly the case in 20 Celsius.

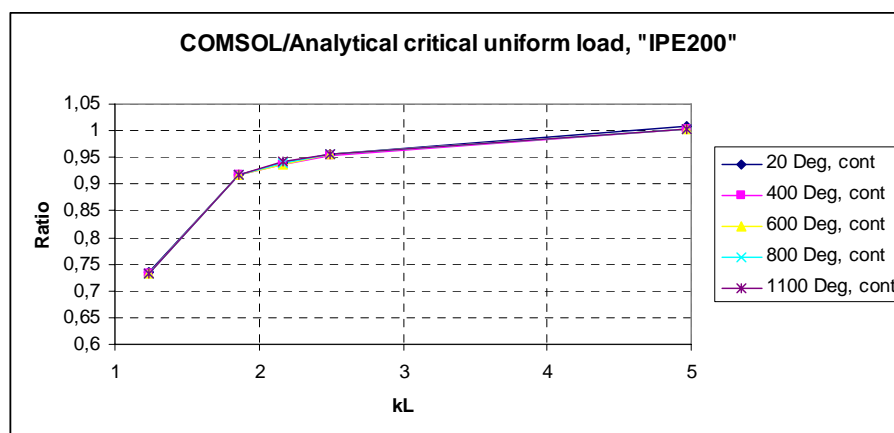


Figure 16. Buckling load ratios for uniform loads, “IPE200”.

In the range of our interest ($kL > 2$) the reduction based on the elastic modulus reduction works well. This means, that the critical loads can be calculated at the ambient temperatures and multiplied by the reduction factor of the elastic modulus according to the temperature in the fire.

Finally some thermal analyses in fire were done to see, how much the uniform temperature profile analysis is on the safe side. “IPE200” profile with the span 4 m and for the uniform load was analyzed. Large displacement theory using the material parameters in fire as defined in [13] was used. The coefficient of heat transfer by convection was $25 \text{ W/m}^2\text{K}$ and the surface emissivity of the steel member 0.7.

The initial imperfections to the analysis were given by the constant horizontal load acting at the top flange of the beam. The quantity of this uniform load was defined to give the horizontal displacement $L/1000$ at the mid-span of the beam. Figure 17 illustrates this imperfection load.

The thermal analysis was done using the ISO fire as the gas temperature around the entire beam. The uniform vertical load for the beam was that defined in the previous uniform temperature profile analysis for different temperatures (400, 600, 800 1100 °C) as a buckling load. The idea was to calculate the collapse time for the buckling loads in the ISO fire. Figures 18 and 19 illustrate the displacements in one case: temperature 400 °C and the linear buckling load 13.35 kN/m.

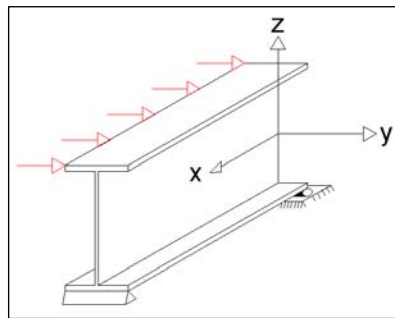


Figure 17. Imperfection load for the large displacement theory.

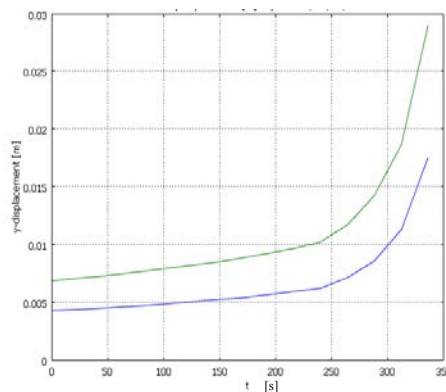


Figure 18. Horizontal displacements (Lower: centroid, upper: top flange mid span) for “IPE200, span 4 m, load 13.35 kN/m

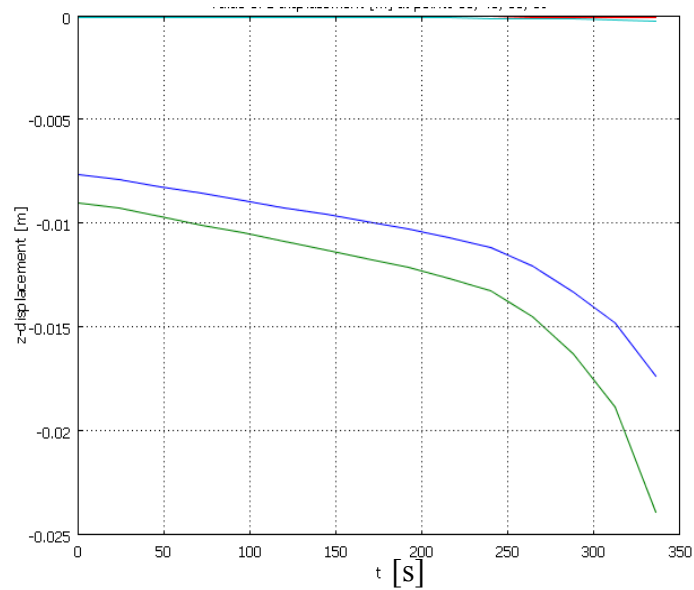


Figure 19. Vertical displacements (upper: centroid, lower: top flange mid span) for “IPE200, span 4 m, load 13.35 kN/m.

The time when no convergence was found for this case was 336 s (5.6 min). The maximum surface temperature was then 605 °C and the minimum 496 °C. Table 3 illustrates the similar results for other cases.

The displacement response curves were similar to Figures 18 and 19 in all the cases considered without end plates.

Table 3. Critical times and temperatures at transient analysis.

T °C	q_{cr} (kN/m)	t_{cr} (s)	T_{max} °C	T_{min} °C
400	13.35	336	605	496
600	5.912	408	676	563
800	1.716	720	895	785
1100	0.429	1512	1155	1094

Solutions with end plates in ambient conditions

In this case the previous fork supported analysis model is modified by adding end plates to the both ends of the beam. The end plates were modeled so, that they were fixed to the both flanges and to the web. The plates were locating outside the beam span at both ends. Figure 20 illustrates the meshing at the end plates. In the ambient conditions some cases were solved using ABAQUS, but most of the cases were solved using COMSOL.

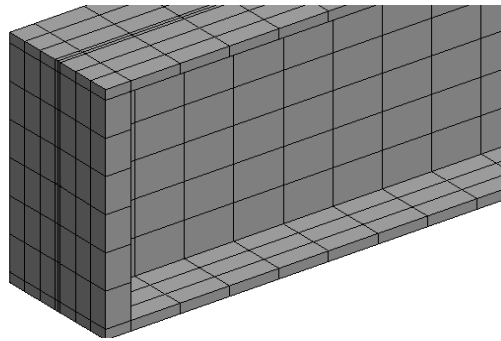


Figure 20. Meshing of end plates, "IPE200", span 4 m, end plate 20 mm.

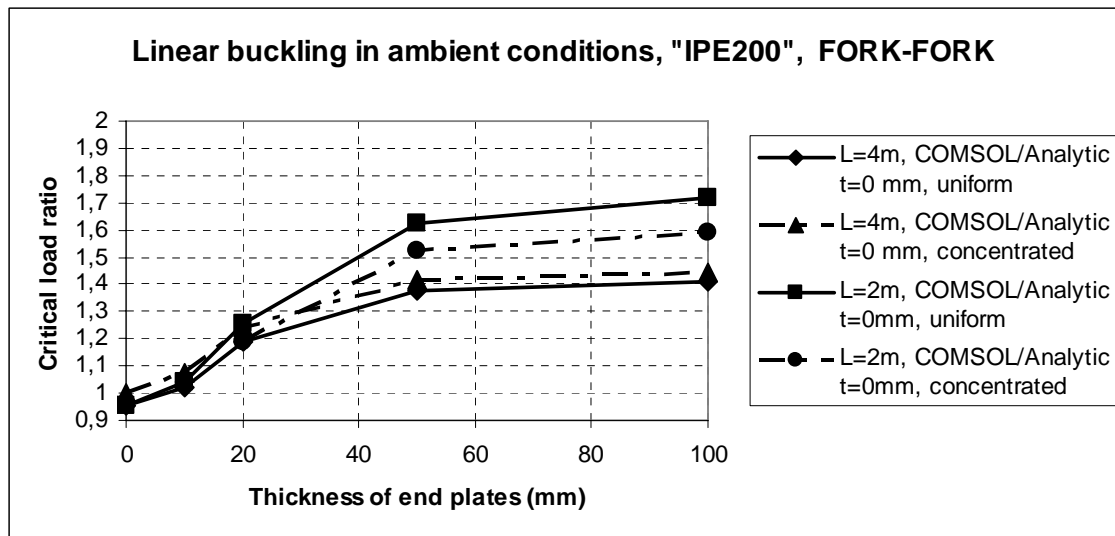


Figure 21. Effect of end plates on the linear buckling loads.

Figure 21 illustrates the results for "IPE200" beam with the spans 2 and 4 m. The critical load ratios shown in the figure are COMSOL critical loads with different end plates versus analytic solutions without end plates.

It can be seen, that the critical lateral torsional buckling load is increasing similar way for uniform and concentrated loads. Using the end plate thickness 20 mm the buckling loads increase about 20 % compared to the solutions without the end plates. Using very thick plates (100 mm) the buckling loads are 1.4-1.7 times compared to the buckling loads without the end plates. Typical end plate thicknesses for IPE 200 profile may be 15 mm and then the increase of the lateral buckling load is about 10 %.

It can be seen, that for the span 2 m ($kL = 2.48$) the increase of the buckling load with very thick end plates is 60-70 %, but for the span 4 m ($kL = 4.96$) it is about 40%. It is clear that when the parameter kL increases to 5 and above, then the effect of the end plates is decreasing, because the effect of the warping is decreasing generally. However, in the range 2 - 5 the end plate effect is 40 - 70 % in maximum. The very thick plate may simulate the stiffness of the joint including end plate bolted to the column flange with stiffeners at the column web or some other cases.

The effect of the boundary conditions is very important. Fig. 22 shows the results for "IPE200" with the span of 4 m, with the left support being fork support and right support being fixed support as shown in Figure 9 c.

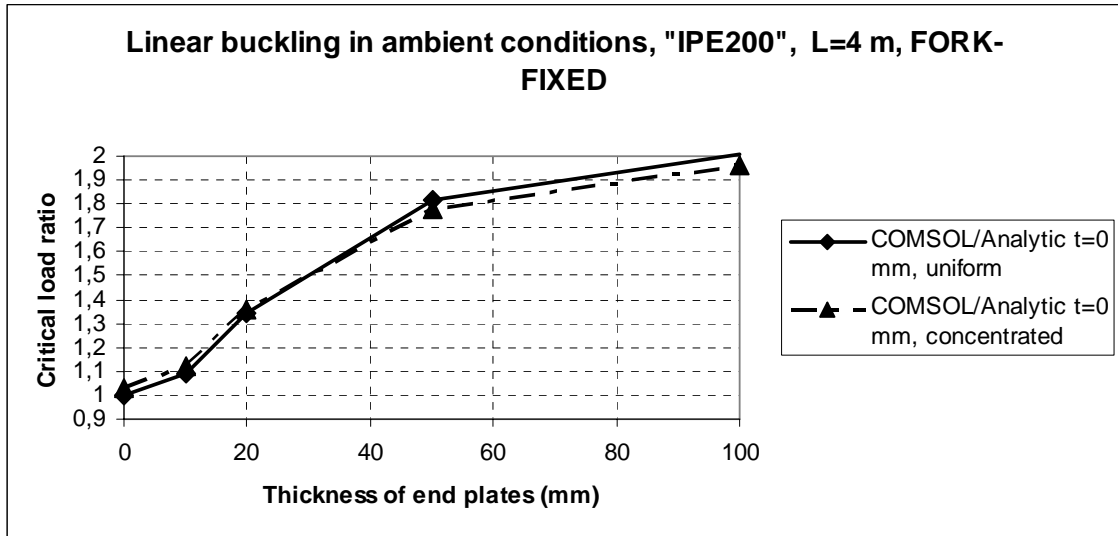


Figure 22. Effect of end plates on the linear buckling loads for other boundary conditions.

It can be seen, the effect of the end plates in this case is double in maximum comparing to Figure 21. Also with the end plates, the buckling mode is approaching the distortional mode when the torsional parameter kL is getting smaller.

Solutions with end plates in fire conditions

The uniform temperature profile analysis gave (mean of proportional buckling loads of all cases for “IPE200” beams 1.013) the same results as it was obtained earlier by reducing the elastic modulus according to the temperature. The buckling modes for large kL values were clearly the lateral torsional modes. Examples are shown in Figure 23 for the end plate thicknesses 20 mm.

The thermal analysis showed, as expected, that especially thick end plates are cooler as a whole, so sustaining more stiffness at elevated gas temperatures, than in the uniform temperature profile analysis. Figure 24 illustrates the temperatures of the beam for one case in the ISO fire.

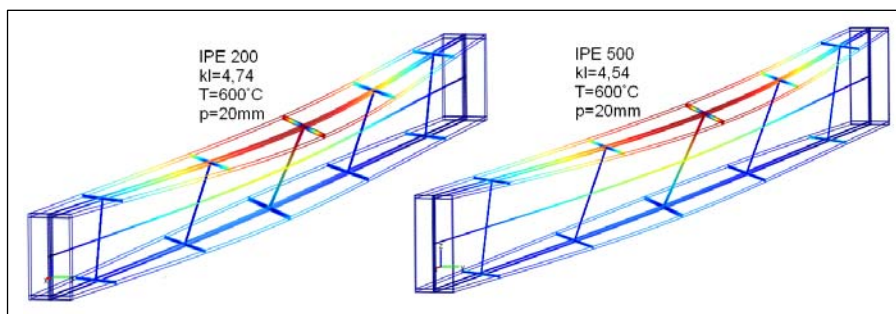


Figure 23. Buckling modes with end plates in fire condition for high kL values.

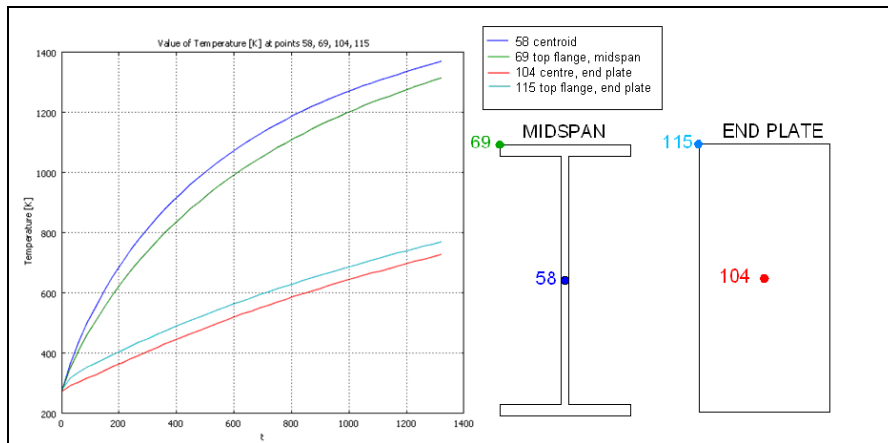


Figure 24. Temperatures versus time, “IPE200”, span 4 m, end plate thickness 100 mm, thermal analysis (COMSOL). The legends for curves from bottom up: 104 (end plate mid), 115 (end plate top), 69 (top flange mid span), 58 (centroid mid span).

The resistance times for “IPE200” beams with the spans 4 m in ISO fire were calculated for different uniform loads using thermal analysis. The load levels were lower than the critical loads for ambient conditions. The loads can be seen at the edges in Fig. 25. The uniform temperature profile analysis gave the reduction of critical loads following the reduction of the elastic modulus as a function of the gas temperature (Figure 7) which is increasing with time following ISO curve. The temperature analysis resistance time was that, when the horizontal displacements were at the “turning” point in Figure 26. Figure 25 illustrates the time increases for different load levels compared to the uniform temperature profile analysis results (E reduction) when the end plate thickness is 10 mm. The load level ratios in Figure 25 means the uniform load (q_{cr}) versus the linear buckling load in the ambient temperature ($q_{cr}(T=20\text{ }^{\circ}\text{C})$).

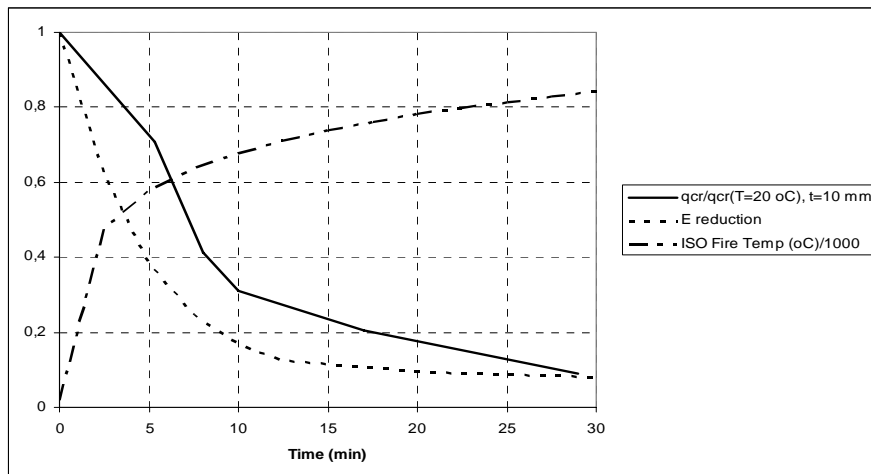


Figure 25. Resistances following thermal and uniform temperature profile analyses.

It can be seen from Figure 25 that the resistance time increases much using the thermal analysis compared to the uniform temperature profile analysis. For example the load level in some cases may be 0.2-0.4 (mechanical load factor ratio in fire versus that in ambient conditions). From Fig. 25 can be seen the increase of the resistance time for the load level 0.2 from about 8 minutes up to about 17-18 minutes. The results were the same for the cases without the end plates. For thicker end plates the increase in the resistance time is larger. The increase of the resistance time in the beginning of the fire is of the most importance when considering the safety of people.

Horizontal and vertical displacements for the load 4 kN/m are given in Figure 26 and Figure 27 for the case 20 mm end plate and 4 m span.

By reading the displacements in Figures 26 and 27 at the time about 1000 s from the start of the ISO fire, the following displaced situation at the mid span can be drawn. It

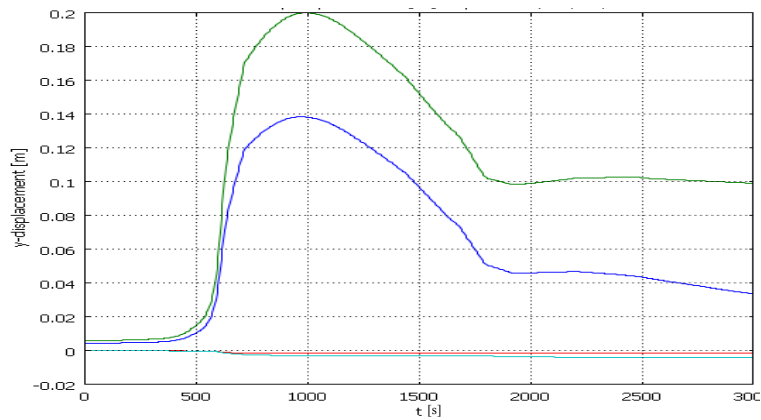


Figure 26. Horizontal displacements of “IPE200” in ISO fire.). The legends for curves from bottom up: end plate top, end plate mid, centroid mid span, top flange mid span.

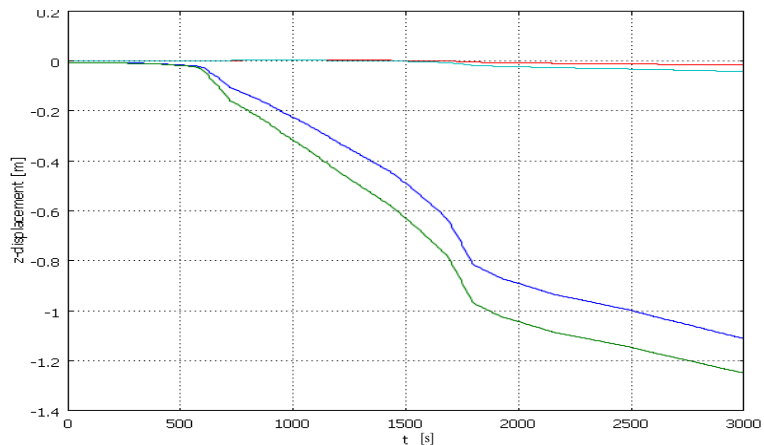


Figure 27. Vertical displacements of “IPE200” in ISO fire. The legends for curves from bottom up: top flange mid span, centroid mid span, end plate top, end plate mid.

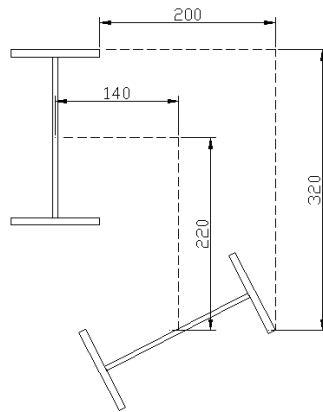


Figure 28. Displacement of “IPE200” from 1000 s (16.7 min) after start of ISO fire.

can be seen from Figure 26 that the horizontal displacements are getting smaller after the stage presented in Figure 28.

It should be noted that so large displacements may happen in fire cases, not at ambient conditions. The unsolved problem in structural mechanics is, as far as known by the authors, the criteria for the collapse of the beam with very large displacements.

Conclusions

The results show the increase of 5-20 % in the buckling loads using typical (10-20 mm) end plates. The buckling loads can be 1.4-1.7 times larger if the end plates are very thick, or generally the joint stiffness in warping is large, compared to the case without end plates. The situation is the same both in ambient and fire situations. The reduction of the buckling load follows the reduction of the elastic modulus at elevated temperatures using the uniform temperature profile analysis, as expected.

The parameter kL was found to be the proper measure when considering different buckling modes. In the cases considered the lateral torsional buckling mode was critical if $kL > 2$. If this parameter is very large, then the role of warping is decreasing, as is known generally.

The considerable increases in the resistance times can be get using the thermal analysis instead of the uniform temperature profile analysis. The criteria to stop the calculations in the thermal analysis are still open.

Acknowledgements

The reviewer of the paper is gratefully acknowledged of the important notes.

References

- [1] Bleich F., *Buckling strength of metal structures*, McGraw-Hill Company, 1952.
- [2] Timoshenko S. P., Gere, J. G., *Theory of elastic stability*, McGraw-Hill, 1961.
- [3] Vlasov V. Z., *Thin-walled elastic beams*, National Science Foundation, Washington (DC), 1959.
- [4] Björk T., On the spring constant in open section joints, *In Proceedings of the 4th Finnish Mechanics Days*, Niemi E. (Ed), Research Papers 17, Lappeenranta University of Technology, Lappeenranta, Finland, 1991, pp. 351-360.
- [5] Krenk S., Damkilde L., Warping of joints in I-beam assemblages, *Journal of Engineering Mechanics*, 117(11), 1991; pp. 2457-2474.
- [6] Tong G. S., Yan X. X., Zhang L., Warping and bimoment transmission through diagonally stiffened beam-to-column joints, *Journal of Constructional Steel Research*, 61, 2005, pp. 749-763.
- [7] Masarina A., The effect of joints on the stability behaviour of steel frame beams, *Journal of Constructional Steel Research*, 58, 2002, pp. 1375-1390.
- [8] Simões da Silva L., Towards a consistent design approach for steel joints under generalized loading, *Journal of Constructional Steel Research*, 64 2008, pp. 1059-1075.
- [9] DIN 18800 Part 2, November, *German Standards – Steel Structures*, 1992.
- [10] DIN 4114, July, *German Standards – Stability Cases*, 1952.
- [11] Heinisuo M., Laine V., Lehtimäki E., Enlargement of the component method into 3D, *Proceedings of Nordic Steel Construction Conference*. Luleå University of Technology, SBI, Publication 181, Malmö, Sweden, September 2-4. 2009, pp. 430-437.
- [12] EN 1993-1-8, Eurocode 3: *Design of steel structures*, Part 1-8: Design of joints, CEN, Brussels, 2005.
- [13] COMSOL *Multiphysics 3.2*.
- [14] ABAQUS STANDARD 9.6.
- [15] EN 1993-1-1, *Eurocode 3: Design of steel structures, Part 1-1: General rules and rules for buildings*, CEN, Brussels, 2005.
- [16] EN 1993-1-2, *Eurocode 3: Design of steel structures, Part 1-2: General rules. Structural fire design*, CEN, Brussels, 2005.
- [17] ANSI/AISC 360-05, *An American National Standard, Specification for Structural Steel Buildings*, March 9, American Institute of Steel Construction, Inc, Chicago, 2005.
- [18] Kirby P. A., Nethercot D. A., *Design for Structural Stability*, Granada Publishing, Suffolk, 1979.

Marco Santarelli
Universita' Politecnica Delle Marche
P:zza Roma 22, 60121 Ancona, Italy
marcosantarellis@yahoo.it

Markku Heinisuo, Ari Aalto
Tampere University of Technology
P.O. Box 600, 33101 Tampere, Finland
markku.heinisuo@tut.fi, ari.aalto@tut.fi